3D Illumination for Inspection of Mechanical Parts

Sahar Ahmadi and Ted Hubbard[1*]
[1]Mechanical Engineering, Dalhousie University, Halifax NS, Canada
*ted.hubbard@dal.ca

Abstract—This paper demonstrates an optical method for inspection of small 3D mechanical parts. A miniaturized USB microscope experimental setup is presented that uses Reflectance Transformation Imaging (RTI) to image mm scale objects. RTI involves the use of multiple LEDs from a range of 3D illumination angles. A sequence of images is taken and can be combined in various forms to achieve a single composite image that emphasizes facets orientations and shadow locations. The paper describes the experimental setup required to take such images: including LED light sources, Arduino microcontroller and MATLAB controlling software. Sample images from multiple objects are shown, as well as resultant three dimensional information.

Keywords; imaging, Reflectance Transformation Imaging, camera

I. INTRODUCTION

The information an image provides depends on the lighting conditions in use. For 3D objects different aspects of the three dimensional shape can be imaged either by rotating the camera position, using multiple cameras (for example stereoscopic cameras), or rotating the sample as is done on some 3D scanners. In this paper we examine the case where imaging is limited to a single camera from a single orientation: for example, large or very small parts may not be able to be rotated with respect to the camera. The use of multi-angle illumination allows for the extraction of 3D information from fixed orientation 2D images.

Although there are many different ways of illuminating and imaging objects, the most common techniques involve fixed illumination from a fixed camera orientation. Standard digital photography typically captures images in coaxial (or near coaxial) illumination conditions, in which light beams hit the object surface perpendicular (or nearly so) to the object plane. Hence, three-dimensional surface features such as texture details or elevation differences are not easily discerned. The two main types of reflection illumination are: 1) inline illumination involving a beamsplitter in the optical light path, and 2) ring illumination. In the case of inline illumination, the sample is lit along the optical axis, producing bright regions on flat parts of the sample and dark regions on sloped parts of the sample. Ring illumination is typically close to the optical axis and produces similar results without the added complexity of the internal beamsplitter.

Multi-angle illumination has been used in other fields particularly in archeology, where it is often called Reflectance Transformation Imaging (RTI) or Polynomial Texture Mapping (PTM). RTI captures multiple images under various lighting directions, while the camera is fixed orthogonally above the object surface [1]. Topographical and geometrical features of the surface such as texture, surface anomalies and slope can be investigated by analyzing the reflections of the incident light from the surface. For instance, Altshuler and Mannack [1] imaged worn letters, invisible through standard photography, of an inscription from Ephesus as well as an ancient silver tablet. Florindi *et al* [3]applied RTI to detect marks and traces on the surface of a Paleolithic digging stick replica. Payne considered the advantages of RTI in comparison to 3D laser scanning and CT scanning, in terms of producing interactive, customized high-resolution images while being affordable and non-invasive. Miles *et al* [5] imaged an Easter Island statue and made a comparison between photogrammetry, laser scanning and RTI.

RTI has also recently been used for failure studies in engineering. Coules *et al* [6] used RTI to characterize the appearance of failure surface features. RTI as well as specular enhancement were used to enhance the visibility of failure surfaces of a high-strength steel spring and threaded connectors. Lemesle *et al* [7] characterized worn ceramic composite surfaces using surface reflectance.

Many of the above listed RTI apparatus share a number of common factors: i) they utilize digital cameras for imaging which limits maximum magnification, ii) the light source and camera distances are relatively large (10's of cm to 1m), and iii) the image capture and processing is typically done using software specifically designed for RTI or PTM analysis [8, 9].

The objective of this paper is to use RTI techniques, but at a smaller scale with a USB microscope, to better image mm scale 3D mechanical parts. By using a microscope instead of the more typical RTI camera and a miniaturized LED setup it is possible to achieve cm scale working distances, cm scale field of views and sub 0.1 mm resolutions. This high resolution would permit 3D inspection of mm scale parts that would typically only be observed in a planar overhead view. Additionally, custom image processing software is developed to allow further control of image characteristics.

I. EXPERIMENTAL SETUP

Different features of the imaged object can be captured by illuminating the object from various angles. Surfaces that would not be exposed to light in coaxial illumination, can be illuminated with angled light sources and elements can be emphasized through shadows and highlights. The reflected light from a surface depends both on the surface orientation and its surface roughness characteristics. At each location on a surface, there is a surface normal and the brightest state of each location occurs when the illumination is parallel to the surface normal. For a smooth surface, the incident light may have only a single outgoing reflection, while a rough surface scatters the incident light at various angles.

There are a number of ways to distribute N light sources on a hemisphere. In spherical coordinates we define two angles: θ the angle in the XY plane, and ϕ the angle from the Z axis. We can also think of the sphere as a globe with north up, south down and the equator in the middle: θ = longitude and ϕ = 90° -latitude. To achieve equidistribution of sources we should not place the sources at equal increments of θ and ϕ. Doing so would produce a dense packing at the poles and a sparse packing at the equator. Deserno [10] presents an algorithm for determining θ placement at specific ϕ to achieve equal distribution of points. Figure 1 shows N = 50 in 4 bands of latitude from $\phi = 73°$ to 25° with 18, 15, 11 and 6 sources, which produce a more uniform distribution.
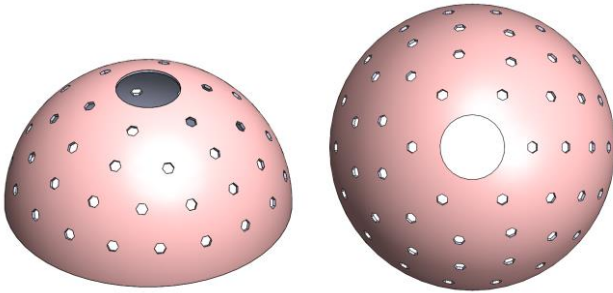

Figure 1. Equidistribution of N sources on a hemisphere. N = 50 with 4 ϕ bands of 18, 15, 11 and 6 θ sources.

To provide the illumination, an Adafruit Soft Flexible Wire NeoPixel Strand - 50 (Product ID: 4560) was chosen. Flexible strand LEDS were chosen as a LED strip would have been difficult to form into a hemisphere. Each Neopixel LED is an individually addressable RGB LED, although all experiments were carried out in white light. A 150 mm diameter hemisphere was 3D printed in PLA, with a shell thickness of 2 mm. 50 holes were placed in the hemisphere according to the placement algorithm outlined above. 8 hours were required to print the shell. The interior of the 3D printed shell was spray painted flat black. Each LED was manually hot glued in place and the excess strand was also hot glued to the shell. Figure 2 shows the resultant shell.

The Neopixels were controlled using an Arduino Uno microcontroller. The sequence of LED lighting is determined by a MATLAB program; alternate programming languages such as Octave could also have been used. Images are taken using a USB microscope (Celestron 44308 Digital Microscope Pro). MATLAB includes libraries for the Arduino microcontroller, the Neopixels, and USB webcams. The MATLAB program lights the first LED, takes a camera image, saves the image, then repeats this for subsequent LEDs. The resultant sequence of images is loaded into another MATLAB program, in this case an image viewer. The N images are divided to N_ϕ bands of ϕ, each with N_θ θ images. The viewer loads the images and saves them in a five dimensional stack of images as shown in Figure 3 (5D = x, y, θ, ϕ, RGB color).

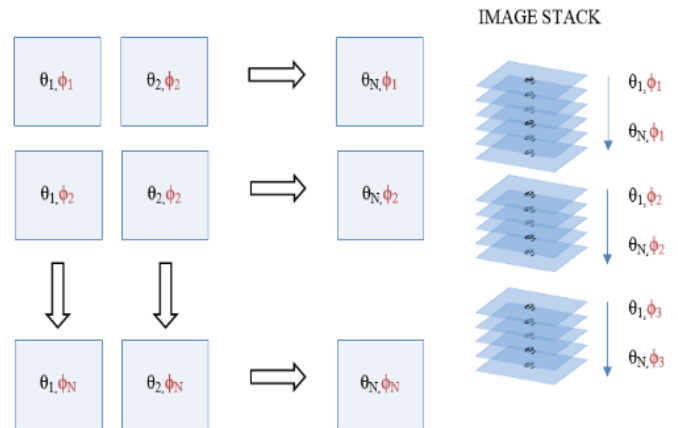Figure 2. USB microscope above 150 mm diameter 3D printed hemisphere with N = 50 Neopixel strand.

Figure 3. Matlab Image stack.

The user can select different images by moving through the image stack, changing either θ or ϕ or both. The MATLAB program can also process the images in a number of ways: average images within the stack, find the difference between images, or find which image produces the maxima intensity at each pixel. The image processing can be used to determine 3D information such as surface orientation. Examples are shown in the next section.

II. RESULTS

As a first example, three irregular but roughly spherical beads ranging in size from 4 mm to 6 mm were imaged. Figure 4 shows the image where all lighting sources are averaged, simulating overhead lighting, although some slight shadowing can be seen. The image field of view in this case was ~2x1.5 cm and the pixel size was 15 μm (0.015 mm). The MATLAB program allows the user to show either the average image, the image from any particular orientation or a weighted sum of both. The average image has less camera noise because all light sources are used as opposed to only 1 source, while the directional image shows higher contrast. Typically, images are displayed in a 50/50 weighted sum of average image and directional image. Figure 5 shows the weighted illumination from one angle, in this case $\phi = 25°$ and $\theta = 0°$ ($\theta = 0°$ at bottom of images). Note in the upper left corner a small indicator showing the light position with respect to the image. Figure 6 shows 6 different illumination directions. In the left column going from top to bottom ϕ is varied from 25° to 57°. In the right column θ is increased from 60° to 180°.

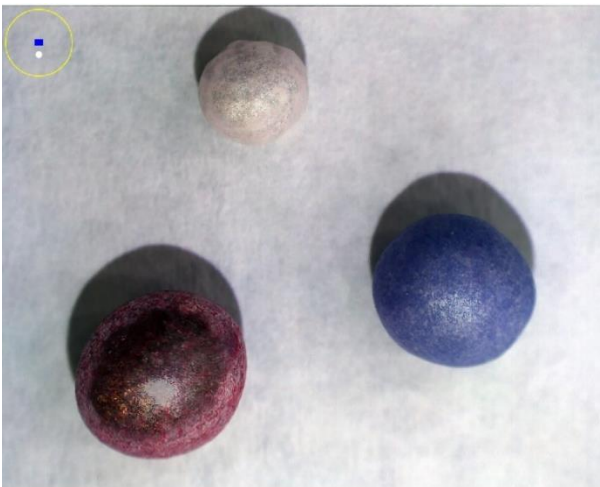Figure 4. Three small irregular beads. White bead is ~4 mm in diameter, red bead ~6mm. Background is a sheet of paper.

Figure 5. Same three beads illuminated from $\phi = 25°$ and $\theta = 0°$. Note lighting indicator at top left.

$\phi = 25°, \theta = 0°$ $\phi = 25°, \theta = 60°$

$\phi = 41°, \theta = 0°$ $\phi = 25°, \theta = 120°$
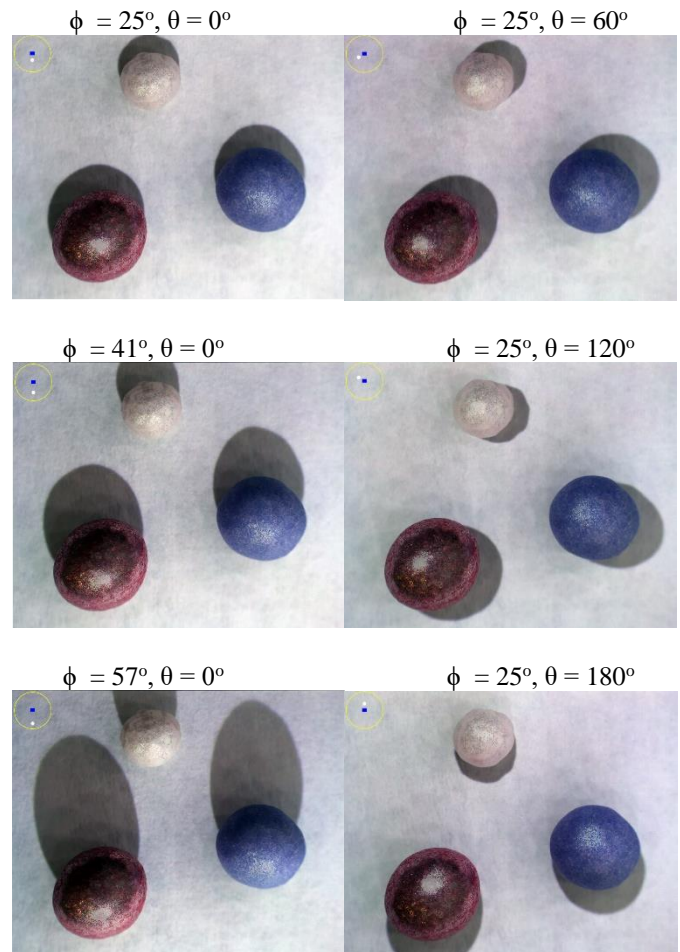
$\phi = 57°, \theta = 0°$ $\phi = 25°, \theta = 180°$

Figure 6. Beads illuminated from different angles. Left column: varying ϕ. Right column: varying θ ($\theta = 0°$ at bottom of images).

III. 3D INFORMATION

Information about the three dimensional shadows can be obtained by finding the minimum and maximum intensities vs. angle. This is done by considering only the top ϕ band of illumination. As these sources are near the vertical axis, flat areas will show little variation other than that caused by shadows. Firstly, the maximum of each pixel is found vs. angle θ. Secondly the minimum of each pixel vs. angle θ is found. Next the difference is found: Δ = max - min. Flat un-shadowed areas will show little Δ. To make the shadows show as dark and the background show as light, (1- Δ) is plotted.

Figure 7 shows the shadow-gram of the beads, showing sixfold shadows caused by the six uppermost light sources. Note that the largest bead casts larger shadows than the smaller beads as it is taller. Note also the sixfold pattern on the top of the largest bead. In this case the top of the bead has 6 bright specular reflections that cause a difference between maximum and minimum and thus show up as black.

Further three dimensional information can be obtained by determining which LED orientation produces the highest intensity on each individual pixel.
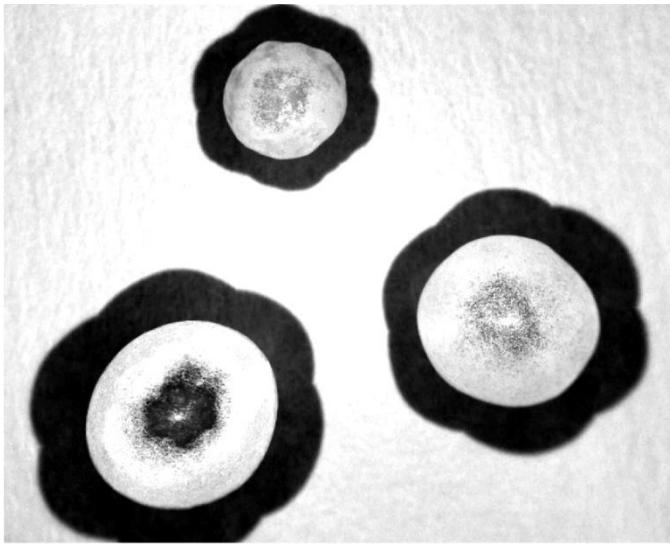
Figure 7. Shadow-gram of 3 irregular beads.

The maximum light intensity orientation corresponds to the local normal of the surface. Firstly, the value of Δ is calculated for each pixel. A user settable threshold sets all flat pixels with $\Delta <$ threshold as grayscale. For each remaining non-flat pixel, the θ and ϕ that produce the maximum intensity are recorded and are plotted as an HSV image, with the hue H given by the value of θ, the saturation S given by the angle ϕ, and value V is set to 1. A small HSV color indicator is located in the upper left of the image. Red indicates light coming from the right or east, green indicates light coming from the northwest and blue indicates light coming from the southwest. The saturation (whether the color is deep and vivid or pale and closer to the white) indicates whether it is a high or low ϕ. Higher saturation corresponds to the larger ϕ (grazing illumination) and lower saturation corresponds to lower ϕ closer to the vertical. Figure 8 shows the HSV normal diagram for the beads.
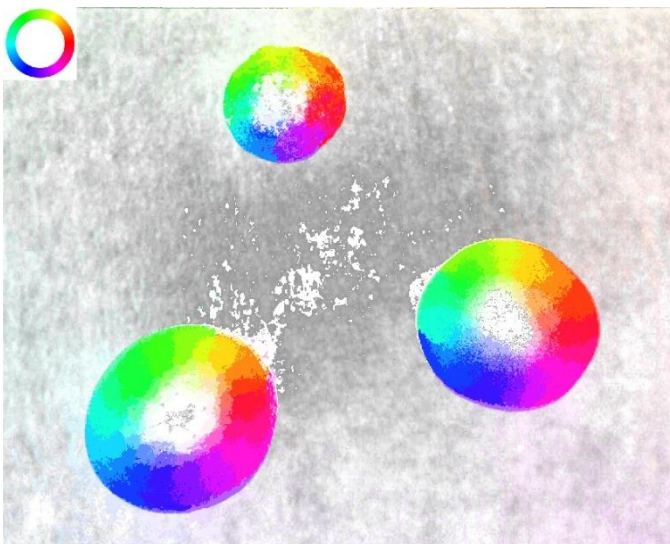

Figure 8. HSV color normal diagram for beads. Hue indicates θ, Saturation indicates ϕ.

Figure 9 shows a second sample, a small chain with 8 mm links. Note that in the original average image (Top) it is difficult to determine the three dimensional location of the links. In the Middle Shadow-gram the shadows indicate the relative height of different parts of the image. For example, the third link from the left is tilted out of plane, it is low at the top high at the bottom and this is indicated by the short shadow on the top and the much longer shadow on the bottom., The HSV normal diagram (Bottom) also shows the 3D orientation of the links. Note the green and purple banding of the third link with the green on top and the purple glow indicating the tilt of the link.
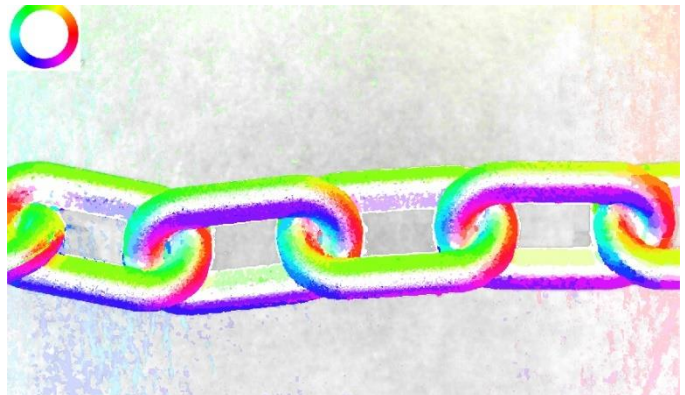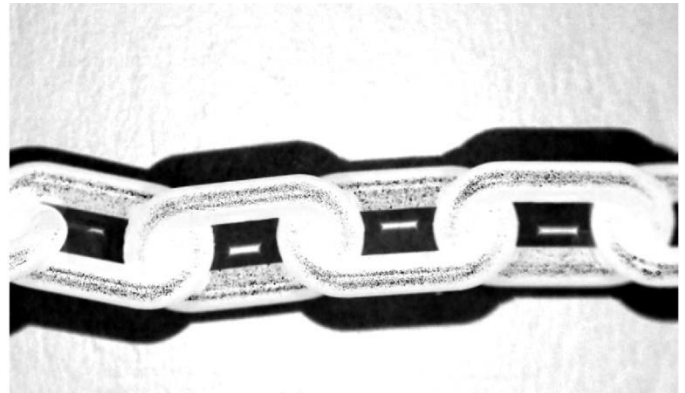

Figure 9. Small plastic chain, 8 mm links. Top: average image, Middle: shadow-gram, Bottom: HSV normal image.

Figure 10 Top shows a small plastic building block. The block consists of a 7.8 mm square base that is 3.1 mm thick. On top of the square base are four 2.5 mm diameter vertical cylinders for a total height of 4.8 mm. On the left of the block is a 4 mm ball joint connect to the block by a filleted horizontal cylinder. Figure 10 Bottom shows the HSV normal image, indicating the ball joint as well as the fillet tops of the four vertical cylinders which is not easily discerned from the overhead view. Note also that the small depression at the center of the square block which is indicated in the HSV normal diagram as a circle with flipped colours (red on left, cyan on right).
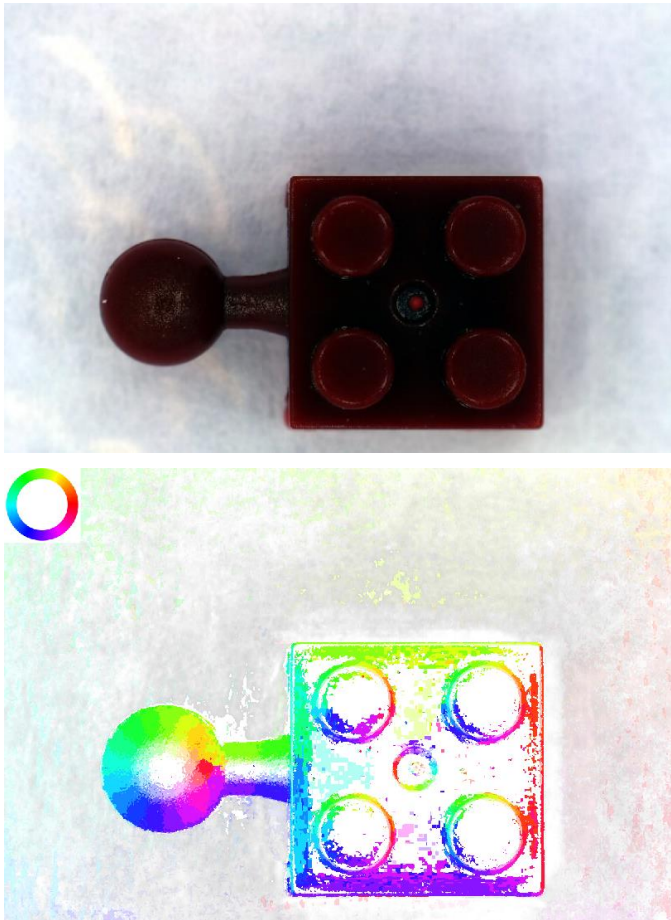

Figure 10. Square plastic block (7.8 mm) with ball joint on left. Top: Average image, Bottom: HSV Normal image.

IV. HEIGHT INFORMATION

It is also possible to extract object heights. The image scale in mm/pixel is calibrated from an object of known size. The user can then select a particular image and draw a line on the image from the start to the end of a shadow. MATLAB uses the *improfile* function to determine the length of the shadow in pixels. From the shadow length, the mm/pixel and the tan of ϕ, MATLAB calculates the height that would produce this shadow. Figure 11 Top and Middle show the block with ball joint illuminated from two different ϕ values. Note the increasing shadow length with increasing ϕ. In the second

image the shadows of the vertical cylinders are also much taller. Figure 11 Bottom shows the user selected shadow and the calculated height. In this case height = 3.2 mm (actual = 3.1 mm measured using digital calipers.) The measured values ranged from 3.0 to 3.2 mm depending on the ϕ chosen and the user selection of shadow end/start pixels, which corresponds to a repeatability of $\pm 3\%$.
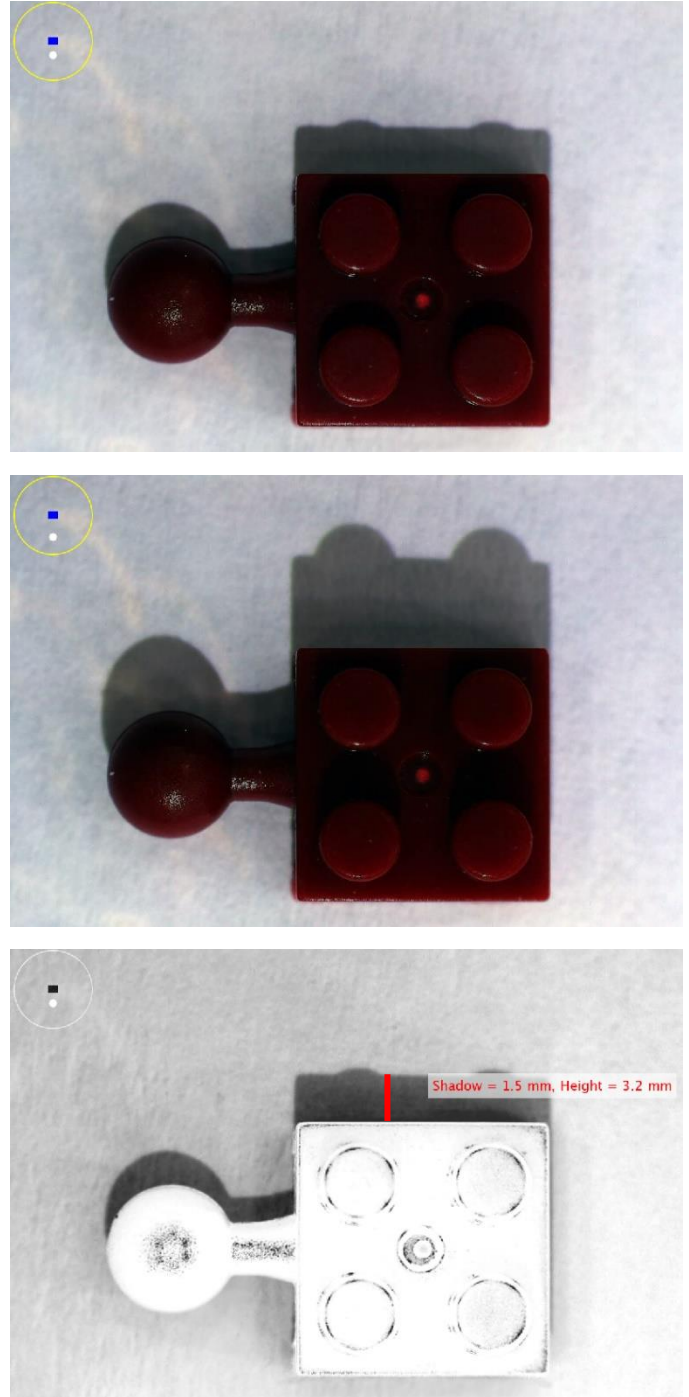

Figure 11. Square plastic block (7.8 mm) with ball joint on left. Top: $\phi = 25°$, Middle: $\phi = 41°$, Bottom: User selection of $\phi = 25°$ shadow edges and calculated height.

As another example a part was CNC milled from HDPE. A 1/8" ball end mill was used to mill two 4 mm circular features 10 mm apart. Figure 12 Top shows the image obtained using conventional lighting. The horizontal scallop lines caused by the ball mill can be seen. However, the true nature of the features is only revealed in Figure 12 Bottom, where low elevation 3D illumination reveals that the circular features are in fact not circles or cylinders but 2 cones of different heights. Using the shadow measurement technique described above, the heights of the cones were correctly measured to be 3.5 mm ± 1 mm on the left and 2.4 mm ±1 mm on the right.
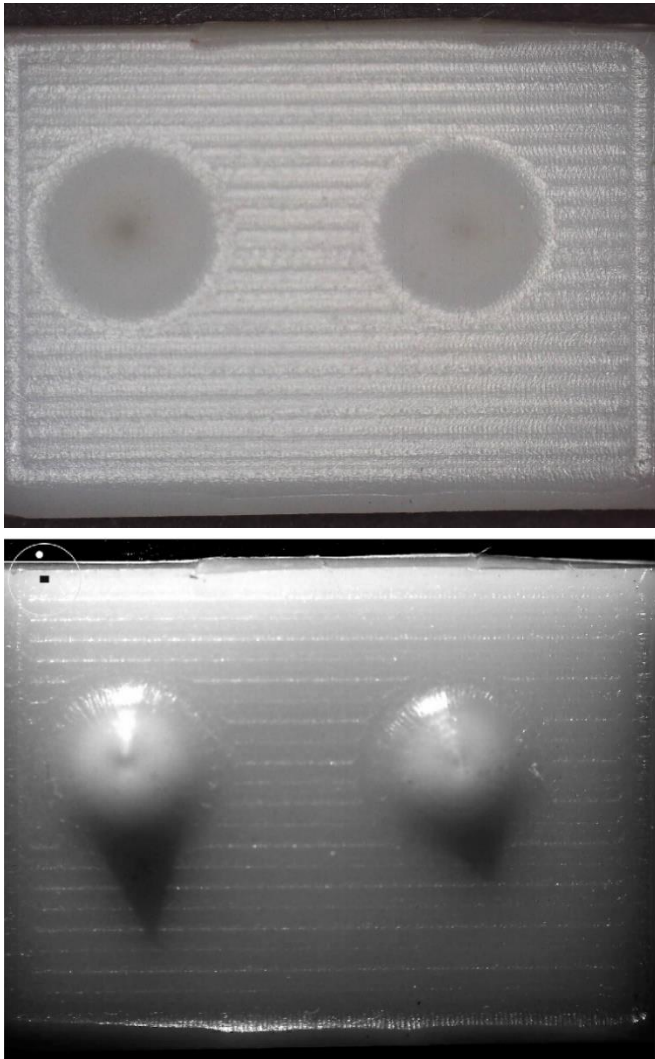

Figure 12. Two 4 mm diamter CNC milled circular features. Top: Image taken using standard illumination. Bottom: Image taken at low elevation 3D lighting, showing two different conical shadows.

V. CONCLUSIONS

We have described an imaging technique using multi-source illumination. This is useful for objects that do not provide 3D information using conventional illumination or are not directly accessible for 3D scanning or viewing from other angles.

In place of flat images taken with conventional lighting, Reflectance Transformation Imaging (RTI) provides orientation selectable images that provide a better understanding of the shape and texture of the object. Addressable LEDs were used in conjunction with an Arduino microcontroller and a MATLAB program to illuminate the object from different angles. The average of all illumination sources produces a brightfield image similar to conventional imaging. The software allows the user to view the sample from different lighting orientations and to combine different weights of the average image with individual lighting orientations in order to highlight different surface features. Information about the surface normals can be obtained by finding the brightest state of each pixel and assigning HSV colors. In addition, the height of objects in the image can be determined by measuring the length of the shadows and the angle of the light.

In conclusion, this paper presented a compact USB microscope and LED setup capable of applying RTI imaging methods to smaller scales to better image mm scale 3D mechanical objects. Microscope images were obtained with field of view of ~1-2 cm and resolutions of 15 μm.

REFERENCES

[1] B. Altshuler and T. Mannack, "Shedding new light on ancient objects," Arion: A Journal of Humanities and the Classics, vol. 22, no. 1, pp. 53-74, 2014. DOI: 10.2307/arion.22.1.0053

[2] G. Pitard, G. Le Goïc, A. Mansouri, H. Favrelière, S. F. Desage, S. Samper and M. Pillet, "Discrete modal decomposition: a new approach for the reflectance modeling and rendering of real surfaces," Journal of Machine Vision and Applications, vol. 28, no. 5-6, pp. 607-621, 2017. DOI: 10.1007/s00138-017-0856-0

[3] S. Florindi, A. Revedin, B. Aranguren and V. Palleschi, "Application of reflectance transformation imaging to experimental archaeology studies," Journal of Heritage, vol. 3, no. 4, pp. 1279-1286, 2020. DOI: 10.3390/heritage3040070

[4] E. M. Payne, "Imaging techniques in conservation," Journal of Conservation and Museum Studies, vol. 10, no. 2, pp. 17-29, 2012. DOI: 10.5334/jcms.1021201

[5] J. Miles, M. Pitts, H. Pagi and G. Earl, "New applications of photogrammetry and reflectance transformation imaging to an Easter Island statue," Journal Antiquity, vol. 88, no. 340, pp. 596-605, 2014. DOI: 10.1017/S0003598X00101206

[6] H. E. Coules, P. J. Orrock and C. E. Seow, "Reflectance transformation imaging as a tool for engineering failure analysis," Journal of Engineering Failure Analysis, vol. 105, pp. 1006-1017, 2019. DOI: 10.1016/j.engfailanal.2019.07.037

[7] J. Lemesle, F. Robache, G. Le Goic, A. Mansouri, C. A. Brown and M. Bigerelle, "Surface reflectance: an optical method for multiscale curvature characterization of wear on ceramic–metal composites," Journal of Materials, vol. 13, no. 5, pp 1024, 2020. DOI: 10.3390/ma13051024

[8] Cultural Heritage Imaging, RTIBuilder and RTI Viewer [Computer software]. Available: http://culturalheritageimaging.org/What_We_Offer/Downloads/

[9] HP Labs, PTM Builder [Computer software]. Available: https://www.hpl.hp.com/research/ptm/HighlightBasedPtms/index.html

[10] M. Deserno, "How to generate equidistributed points on the surface of a sphere," Max Planck Institute for Polymer Research, pp. 99, 2004.